International Journal of Thermophysics (2024) 45:46
https://doi.org/10.1007/s10765-024-03339-x

Measurement of Diffusion Coefficients in Binary Mixtures and Solutions by the Taylor Dispersion Method

J. P. Martin Trusler[1]

Received: 31 December 2023 / Accepted: 5 February 2024 / Published online: 24 February 2024

Abstract
The theory and application of the Taylor Dispersion technique for measuring diffusion coefficients in binary systems is reviewed. The theory discussed in this paper includes both the ideal Taylor–Aris model and the estimation of corrections required to account for small deviations from this ideal associated with a practical apparatus. Based on the theoretical treatment, recommendations are given for the design of practical instruments together with suggestions for calibration, data acquisition and reduction, and the rigorous estimation of uncertainties. The analysis indicates that relative uncertainties on the order of 1% are achievable in practice.

Keywords Binary mixtures · Mutual diffusion · Taylor Dispersion apparatus · Tracer diffusion

1 Introduction

The Taylor Dispersion or chromatographic broadening technique is a well-established means of measuring mutual diffusion coefficients in binary mixtures. In this method, a homogeneous mixture or solution passes through a long tube in steady laminar flow. Into this flow is injected a small aliquot of the mixture or solution having a slightly different composition to that of the mobile phase, thereby creating a region of inhomogeneous concentration that propagates downstream. As a result of advection and diffusion, this concentration distribution develops into a Gaussian function of the distance from the point of injection, the dispersion of which is precisely related to the mutual diffusion coefficient. In a practical experiment, a chromatographic injection valve is used to inject the aliquot, the amount being determined

Special Issue on Transport Property Measurements in Research and Industry: Recommended Techniques and Instrumentation.

✉ J. P. Martin Trusler
m.trusler@imperial.ac.uk

[1] Department of Chemical Engineering, Imperial College London, London SW7 2AZ, UK

by the volume of the installed sample loop. A diffusion tube of circular cross-section is installed in a thermostat and the concentration of the exiting fluid is measured as a function of time with a suitable chromatographic detector. The method is rigorously described by a mathematical model which may be used to obtain the mutual diffusion coefficient from the experimental concentration–time data.

The Taylor Dispersion method is versatile in relation to the types of binary mixtures or solutions that can be studied. The mobile phase can be a liquid [1–3] or a supercritical fluid [4–6]; it can be a solution or a mixture provided that it is homogeneous under the conditions of the experiment. Often, the mobile phase is a pure fluid and the injected phase is a dilute solution of a single solute [7–9]. In this case, the quantity measured is the tracer diffusion coefficient of the solute. For binary systems that are homogeneous over the entire composition range, the composition of the mobile phase is unrestricted and one can measure the mutual diffusion coefficient over the full composition range. The method may also be applied to low-pressure gases (for example, see reference [10]), although such applications are not considered explicitly in this article.

2 The Taylor–Aris Theory

2.1 Fast, Slow, and Intermediate Diffusion

Before introducing any detailed mathematical models, it is useful to consider the expected behavior in limiting cases and for a typical scenario. Consider the mobile phase to be a pure solvent passing through a tube of length L_0 and radius R_0 at a volumetric flow rate $\dot{V}$.[1] In this case, the superficial fluid velocity $\overline{u}_0$ (the velocity averaged over the cross-section) is

$$\overline{u}_0 = \dot{V}/(\pi R_0^2) \tag{1}$$

and solute that passes through the tube at this superficial velocity would elute at time

$$\bar{t}_0 = L_0/\overline{u}_0 = V_0/\dot{V}, \tag{2}$$

where $V_0 = \pi R_0^2 L_0$ is the internal volume of the tube. In laminar flow, the velocity profile over the cross-section of the tube is

$$u(r) = 2\overline{u}_0(1 - r^2/R_0^2), \tag{3}$$

where r is the radial co-ordinate. It is also convenient to define the mean concentration of solute over a cross-section $\overline{c}(z,t)$ as a function of the distance z downstream of the injector and the time t since injection of the solute. It is assumed that the detector measures this mean concentration at $z = L_0$, designated $\overline{c}_L(t)$.

[1] Subscript 0 is used to denote quantities associated with the diffusion tube or the flow within it.

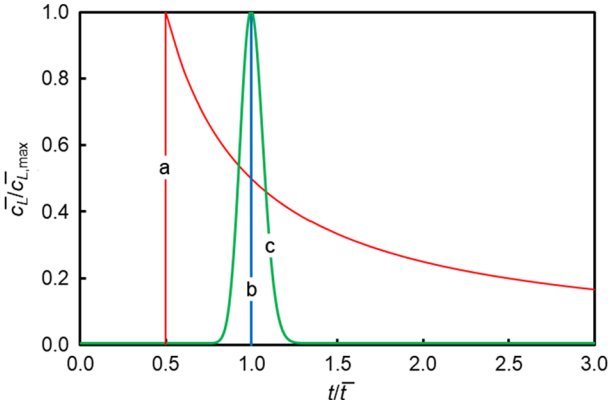

Fig. 1 Relative solute concentration $\bar{c}_L/\bar{c}_{L,\max}$ as a function of relative time $t/\bar{t}$, where $\bar{c}_L$ is the mean solute concentration over the cross-section of the tube measured at the $z=L_0$, $\bar{c}_{L,\max}$ is the maximum value of $\bar{c}_L$, $\bar{t} = V_0/\dot{V}$, where V_0 is the volume of the tube and $\dot{V}$ is the volumetric flow rate of the mobile phase. Curves represent: (a) red, slow-diffusion limit; (b) blue, fast-diffusion limit; and (c) green, typical intermediate case (Color figure online)

In the slow-diffusion limit, the tracer diffusion coefficient of the solute tends to zero and transport along the tube is by advection parallel to the tube axis only. In that case, it is easy to show that $\bar{c}_L(t)$ is zero until time $\bar{t}/2$, at which point it abruptly acquires a finite value that subsequently decays in proportion to $1/t$. The abrupt rise is of course associated with the flat velocity profile near the center of the tube.

A fast-diffusion limit can also be identified in which radial diffusion is sufficiently to homogenize the composition rapid over the small cross-section of the tube, but diffusion in the longitudinal direction is negligible. In that case, the solute pulse does not disperse and simply passes through the tube at the superficial velocity, eluting as a delta function at time $\bar{t}$.

In between these limiting cases, we have a competition between advection which, in the parabolic flow field, acts to disperse the solute axially and diffusion which, in the same flow field, acts to homogenize it radially. The result of this competition is a concentration profile $\bar{c}(z,t)$ that is a near Gaussian function of $(z-\bar{u}_0 t)$ propagating along the tube at velocity $\bar{u}_0$.

Figure 1 illustrates the concentration $\bar{c}_L$ measured at the detector as a function of dimensionless time $t/\bar{t}$ for these three scenarios. Obviously, the interesting one is the intermediate case in which the concentration profile is sensitive to both diffusion and advection.

2.2 Taylor's Solution

The evolution of an axisymmetric concentration distribution $c(r,z,t)$ under steady laminar flow through a circular tube is governed by the advection–diffusion equation:

$$\left(\frac{\partial c}{\partial t}\right)_{r,z} + u\left(\frac{\partial c}{\partial z}\right)_{r,t} = D_{12}\left[\left(\frac{\partial^2 c}{\partial r^2}\right)_{z,t} + \frac{1}{r}\left(\frac{\partial c}{\partial r}\right)_{z,t} + \left(\frac{\partial^2 c}{\partial z^2}\right)_{r,t}\right]. \tag{4}$$

Here, z is the longitudinal co-ordinate, r is the radial co-ordinate, D_{12} is the mutual diffusion coefficient, and $u = u(r)$ is the steady flow velocity parallel to the axis, given by Eq. 3. The concentration is that of one of the two components of the binary mixture or solution and is expressed in molar units. For an impermeable and non-adsorbing wall, the radial boundary condition is

$$\left(\frac{\partial c}{\partial r}\right)_{t,z} = 0 \quad \text{on } r = R_0. \tag{5}$$

In a Taylor dispersion measurement, the initial condition is idealized as follows:

$$c(r, z, t = 0) = c_0 + \left(\frac{n}{\pi R_0^2}\right)\delta(z), \tag{6}$$

where c_0 is the constant concentration of the specified components in the mobile phase entering the tube, n is the excess amount of the specified component present in the injected aliquot, and $\delta(z)$ is the Dirac delta function.

In order to obtain an analytical solution of Eq. 4 subject to the specified boundary and initial conditions, Taylor [11] argued that $(\partial^2 c/\partial z^2)_{r,t} \ll [(\partial^2 c/\partial r^2)_{z,t} + r^{-1}(\partial c/\partial r)_{z,t}]$. Neglecting the former, which effectively discounts axial diffusion, the solution is

$$\bar{c}_L(t) = \left(\frac{n}{\pi R_0^2\sqrt{4\pi K t}}\right)\exp\left[\frac{-(L_0 - \bar{u}_0 t)^2}{4Kt}\right], \tag{7}$$

where K is a dispersion coefficient which Taylor found to be

$$K = \frac{\bar{u}_0^2 R_0^2}{48 D_{12}}. \tag{8}$$

2.3 The Aris Solution

Aris revisited the problem, presenting an essentially-exact analysis based on the evolution of the spatial moments of the distribution about an origin $z_0 = \bar{u}_0 t$ moving along the tube at the superficial velocity [12]. Importantly, this analysis does not depend upon the approximations made by Taylor. It yields a spatial distribution about $z_0 = \bar{u}_0 t$ that (a) approaches normality asymptotically and (b) is characterized by a variance (second spatial moment) that increases almost linearly with time. These statements can be qualified by considering the exact solutions for the second moment and the general behavior of the higher-order moments.

The exact second moment of the distribution averaged over the cross-section of the tube is

$$\nu_2 = 2\left(\frac{\overline{u}_0^2 R_0^2}{48 D_{12}} + D_{12}\right)t - 128\left(\frac{\overline{u}_0^2 R_0^4}{D_{12}^2}\right)\sum_{n=1}^{\infty}\alpha_{0n}^{-8}\left[1 - \exp\left(\frac{-\alpha_{0n}^2 D_{12} t}{R_0^2}\right)\right], \quad (9)$$

where α_{0n} is the n^{th} turning point of the zeroth-order Bessel function of the first kind [13]. Thus, ν_2 comprises three parts: a leading term proportional to time, a constant term, and a transient term which decays exponentially with time. Alizadeh et al. [13] show that the transient term is smaller than 0.01% of the leading term for dimensionless time $\tau > 0.6$, where τ is defined by

$$\tau = D_{12} t / R_0^2 \quad (10)$$

a condition that is readily achieved in practice. Therefore, enumerating $\sum_{n=1}^{\infty}\alpha_{0n}^{-8}$, the second moment reduces to

$$\nu_2 = 2\left(\frac{\overline{u}_0^2 R_0^2}{48 D_{12}} + D_{12}\right)t - \left(\frac{\overline{u}^2 R_0^4}{360 D_{12}^2}\right) \quad (11)$$

which is indeed a linear function of time.[2] Typically, $\overline{u}_0^2 R_0^2 \big/ 48 D_{12} \gg D_{12}$ in which case the ratio of the constant term to the term proportional to time is simply $-1/15\,\tau$. Therefore, by a suitable choice of experimental parameters, the variance can be rendered essentially proportional to time.

The higher moments of the spatial distribution decay with time such that the distribution progressively approaches normality. The rate at which this occurs can be quantified by considering the time evolution of the absolute skewness β, defined as

$$\beta = \nu_3^2 \big/ \nu_2^3, \quad (12)$$

where ν_3 is the third moment of the distribution about z_0 averaged over the cross-section. This has been studied in detail by Chatwin [14], leading to the following asymptotic expression for the absolute skewness:

$$\beta = 3/(50\tau). \quad (13)$$

This is typically small but not necessarily negligible; for example, when $\tau = 5$, $\beta = 10^{-2}$. Chatwin's series expansion of the exact solution [14] is very useful for gauging the approach to normality. This will be discussed further below when corrections to the zeroth-order theory are considered. Unfortunately, there is some confusion in the literature concerning the skewness, with Alizadeh et al. [13] stating that β is $< 5 \times 10^{-8}$ under practical conditions, which appears to be incorrect. Aris [12] also gives an expression for β which differs from Eq. 13.

[2] In the original publication of Aris [12], the sign of the second term was positive. This error is corrected in Alizadeh et al. [13].

2.4 The Temporal Distribution

Under the conditions in which both the constant term in Eq. 11 and the third and higher moments of the distribution are negligible, the concentration averaged over the cross-section at $z = L_0$ is given by the following modified Gaussian function:

$$\bar{c}_L(t) = \left[\frac{(n/V_0)}{\sqrt{2\pi(\sigma_0^2/\bar{t}_0^2)(t/\bar{t}_0)}} \right] \exp\left[\frac{-(t-\bar{t}_0)^2}{2\sigma_0^2(t/\bar{t}_0)} \right]. \tag{14}$$

This is characterized to within a constant scaling factor by two parameters:

$$\bar{t}_0 = V_0/\dot{V} \tag{15}$$

and

$$\sigma_0^2 = \frac{2K\bar{t}_0}{\bar{u}_0^2}, \tag{16}$$

where the dispersion coefficient K is

$$K = \frac{\bar{u}_0^2 R_0^2}{48 D_{12}} + D_{12}. \tag{17}$$

Since, $\bar{u}_0 = L_0/\bar{t}_0$, the diffusion coefficient may be determined from σ_0^2 and $\bar{t}_0$ plus the length and volume of the diffusion column according to the quadratic relation:

$$\sigma_0^2 = \frac{V_0\bar{t}_0}{24\pi L_0 D_{12}} + \frac{2D_{12}\bar{t}_0^3}{L_0^2}. \tag{18}$$

Here, the second term on the right is the small axial dispersion term neglected by Taylor; neglecting that term, $D_{12} \approx V_0\bar{t}_0/\left(24\pi L_0\sigma_0^2\right)$. Note that elimination of $\bar{u}_0$ in favor of $L_0/\bar{t}_0$ eliminated $\dot{V}$ from the working equation.

Equations 14 and 18 comprise the working equations of the idealized Taylor–Aris model.

3 Corrections to the Idealized Taylor–Aris Model

The idealized model defined above provides a very convenient starting point. Of course, a practical instrument will differ (usually slightly) from this idealized model in several respects. When, as should be the case in a well-designed instrument, departures from the idealized Taylor–Aris model are slight, a first-order perturbation treatment as outlined here will be sufficient. The perturbations to be considered

include the finite volumes of the injection loop and detector, the finite concentration perturbation, the finite length of the diffusion column, non-uniform and/or non-circular cross-section of the column, any abrupt changes in diameter where tubing runs join, coiling of the diffusion column, and the presence of additional inlet and outlet tubing runs. Some of these factors can be modeled sufficiently well to permit the calculation of corrections; others are difficult to quantify precisely and should be rendered negligible by design.

Corrections and potential systematic errors are most easily analyzed as first-order perturbations to the temporal mean and variance of the distribution. Since Eq. 14 is not purely Gaussian, the parameters $\bar{t}_0$ and σ_0^2 defined above differ from the true temporal mean and variance of the distribution in the idealized Taylor–Aris model. However, as shown by Alizadeh et al. [13], in leading order they differ from those quantities by factors of $(1 + m\zeta_0)$, with $m=2$ for the mean and $m=4$ for the variance, where ζ_0 is a dimensionless quantity given by

$$\zeta_0 = \frac{\dot{V}}{48\pi L D_{12}}. \tag{19}$$

Typically, ζ_0 is of order 10^{-3} or less. Therefore, for the purposes of estimating *small* corrections to the zeroth-order theory, one can treat perturbation to the temporal mean and variance of the distribution as the perturbations to $\bar{t}_0$ and σ_0^2, respectively. In the following, we evaluate or estimate the perturbations $\delta\bar{t}$ and $\delta\sigma^2$ that must be *added* to the zeroth-order expressions for the temporal mean and variance to obtain values correct to first-order. Therefore, these perturbations should be *subtracted* from the experimentally determined temporal mean and variance before evaluation of the diffusion coefficient via Eq. 18. Expressions for the perturbations that can be calculated in practize are collected in Table 1 for ease of reference. Other perturbations considered can only be estimated roughly and should be rendered negligible. In these cases, equations mentioned in the text provide a basis for ensuring this.

3.1 Finite Injector Volume and Finite Concentration Difference

The injection system is typically a tubular sample loop of volume V_{inj} connected to (or a part of) a chromatographic injection valve. Without loss of generality, the internal diameter of the sample loop may be taken as the same as that of the diffusion tube, so that $V_{\mathrm{inj}} = \pi R^2 L_{\mathrm{inj}}$, where L_{inj} is the length of the sample loop. Just after actuation of injection valve, the concentration will display a rectangular distribution with a uniformly elevated concentration of one component between $z=-L_{\mathrm{inj}}$ and $z=0$. The second spatial moment of such a distribution is $L_{\mathrm{inj}}^2 \big/ 12$ and the center of the distribution moves with velocity $\bar{u}_0$; therefore, the corresponding perturbation are as given in Table 1. These results remain valid for sample injection loops that have an inner diameter different to that of the diffusion column provided that the influence of the diameter change is negligible, a criterion that is discussed further below.

Table 1 First-order perturbations to the time and temporal variance parameters $\bar{t}$ and σ^2.[a]

Factor	Time perturbation	Variance perturbation
Injector	$\delta\bar{t}_{\text{inj}} = \frac{1}{2}\left(\frac{V_{\text{inj}}}{\dot{V}}\right)$	$\delta\sigma^2_{\text{inj}} = \frac{1}{12}\left(\frac{V_{\text{inj}}}{\dot{V}}\right)^2$
Detector [b]	$\delta\bar{t}_{\text{det}} = m_1\left(\frac{V_{\text{det}}}{\dot{V}}\right) - m_2\left(\frac{R^2}{48D_{12}}\right)$	$\delta\sigma^2_{\text{det}} = m_3\left(\frac{V_{\text{det}}}{\dot{V}}\right)^2 + m_4\left(\frac{R^2}{48D_{12}}\right)\left(\frac{V_{\text{det}}}{\dot{V}}\right)$
Intercept	$\delta\bar{t}_{\text{int}} = 0$	$\delta\sigma^2_{\text{int}} = \frac{-R^2\sigma_0^2}{15D_{12}\bar{t}}$
Skewness	$\delta\bar{t}_{\text{skew}} = \frac{R^2}{84D_{12}}$	$\delta\sigma^2_{\text{skew}} = \frac{2R^2\sigma_0^2}{103D_{12}\bar{t}}$
Coiling	$\delta\bar{t}_{\text{coil}} = 0$	$\delta\sigma^2_{\text{coil}} = \left(\frac{-\dot{V}}{24\pi L_0 D_{12}}\right)\left(\frac{De^2Sc}{653}\right)^2$
Additional tubing	$\delta\bar{t}_{\text{tube}} = \sum_{i=1}^{n}\left(\frac{V_i}{\dot{V}}\right)$	$\delta\sigma^2_{\text{tube}} = \left(\frac{\pi R_0^4 L_i}{24D_{12}\dot{V}}\right)\sum_{i=1}^{n}\left(\frac{D_{12}}{D_{12}^{(i)}}\right)\left(\frac{R_i}{R_0}\right)^4$

[a]Symbols: V_{inj} = injector volume, $\dot{V}$ = volumetric flow rate, V_{det} = injector volume, R_0 = diffusion column radius, L_0 = diffusion column length, A_0 = cross-sectional area of diffusion column, V_0 = volume of diffusion column, R_k = radius of additional tube k, L_k = length of additional tube k, V_k = volume of additional tube k, D_{12} = diffusion coefficient at column conditions, $D_{12}^{(k)}$ = diffusion coefficient at conditions in tube k, De = Dean number at column conditions, Sc = Schmidt number at column conditions

[b]See Table 2 for coefficient m_1 to m_4

In principle there is another effect associated with the finite concentration difference between the injected aliquot and the mobile phase. In a non-ideal mixture, there is a significant volume change upon mixing which, in principle, could give rise to a flow rate perturbation. This can be quantified if the loop volume, concentration difference, and volume change on mixing are known and can easily be rendered negligible by making the concentration difference small.

3.2 Finite Detector Volume

Typically, the chromatographic detector is a small prismatic or cylindrical chamber through which the column effluent passes. The entrance to this chamber is taken to be at $z = L_0$ and the detector is assumed to measure the instantaneous mean concentration throughout the chamber. The finite residence time within the detector gives rise to additional contributions to the elution time and the temporal moments which can be modeled under different assumptions. The limits of plug flow and perfect mixing within the detector have been studied by Alizadeh et al. [13] and, neglecting terms of $O(\zeta_0^2)$, the results are as given in Table 1. The parameters m_i that appear here depend upon the assume flow pattern and values for the two limiting cases mentioned above are given in Table 2.

Unfortunately, the exact flow conditions in the detector may not be known. Most commonly, the contribution of the detector volume to the variance has been analyzed with $m_4 = 0$, under which assumption $1/m_3$ is reported to be in the range 5 to 6 [15]. Dasgupta et al. [16] studied the detector-induced dispersion experimentally

Table 2 Parameters determining the detector perturbation

Flow condition	m_1	m_2	m_3	m_4
Plug flow	1/2	0	1/12	1
Perfect mixing	1	−3	1	2
Recommended	1/2	0	1/9	1

using a variable path cylindrical diode array detector cell. Under variation of both V_{det} and $\dot{V}$, the additional dispersion in the detector was found to conform to the tabulated expressions and it was reported that, for $V_{\text{det}} \geq 4$ μL, $m_3 \approx 1/9$ [16]. Further analysis of the data for biphenyl solute in acetonitrile indicates that $m_4 \approx 1$ so that, overall, the flow regime appears to be closer to the plug flow limit than to the perfectly mixed scenario, leading to the recommended coefficients provided in the last row of Table 2.

3.3 Non-infinite Length of the Diffusion Column

As discussed in Sect. 2.2, the zeroth-order working equations emerge as the limiting case for a very long diffusion column. The transient terms in the second spatial moment decay extremely rapidly and, by adopting Eq. 17 for the dispersion coefficient, the small contribution of longitudinal diffusion is captured in the zeroth-order model. This leaves the neglected constant term in Eq. 11 and the influence of higher moments of the distribution. The former leads to a slight underestimate of the second moment and the first-order 'intercept' correction is included in Table 1. The effect of the higher moments of the distribution is considered numerically in the Supplementary Information. It is shown there, using Chatwin's series expansion of the exact solution [14] that the relative error incurred in the second moment by fitting the concentration–time distribution with Eq. 14 is $2/(103\tau)$, leading to the skewness correction given in Table 1.

3.4 Non-circular Cross-Section

The case of an elliptical cross-section has been considered by Aris [12] who showed that the dispersion coefficient (ignoring axial diffusion) is given by

$$K = \left(\frac{\dot{V}^2 L_0}{48\pi V_0 D_{12}} \right) \kappa, \tag{20}$$

where A is the cross-sectional area of the tube and κ is a factor determined by the eccentricity of the tube, defined by $e^2 = 1 - b^2/a^2$ where b is the minor diameter and a is the major diameter. The factor κ is given by

$$\kappa = \frac{(1 - e^2 + \frac{5}{24}e^4)}{(1 - \frac{1}{2}e^2)} \tag{21}$$

so that, when the effective value of R_0^2 is eliminated in favor of $V_0/(\pi L_0)$, one obtains

$$K = \left(\frac{\dot{V}^2 L_0}{48\pi V_0 D_{12}}\right)\left(\frac{1 - e^2 + \frac{5}{24}e^4}{(1 - \frac{1}{2}e^2)\sqrt{1 - e^2}}\right). \\ = \left(\frac{\dot{V}^2 L_0}{48\pi V_0 D_{12}}\right)\left(1 + \frac{e^4}{12} + \cdots\right) \tag{22}$$

Therefore, the effects of small smooth departures from circular cross-section are expected to be negligible provided that the tube dimensions are characterized by length and internal volume.

3.5 Variation of the Tube Radius

Neglecting longitudinal diffusion, initial transient terms and the small constant term in Eq. 11, the second spatial moment at time t is $\nu_2 = \overline{u}_0^2 R^2 t/(24D_{12})$. With $\overline{u}_0 = \dot{V}/A_0$ and $t = V_0/\dot{V}$, where A_0 is the cross-section of the column, one finds that the second *volumetric* moment $\chi_2 = \nu_2 A_0^2$ is given by

$$\chi_2 = \left(\frac{\dot{V} V_0}{24\pi D_{12}}\right), \tag{23}$$

which is independent of the tube radius. Therefore, if the tube dimensions are characterized by length and volume, small variations of radius (such that smooth laminar flow is maintained) do not influence the dispersion and can be considered negligible.

The influence of a step change in radius may not be negligible because of phenomena such as poorly swept portions of the tube, for example, at the interior corner formed upon a reduction of radius. This problem is not amenable to an analytical treatment but it has been studied by computational fluid dynamics (CFD) for the case of abrupt 1:2 radius changes [17]. The results show local effects on the solute dispersion which diminish rapidly downstream toward a small and constant asymptotic increment to the second moment. This effect was shown to depend primarily upon the Peclet number, $Pe = 2R\overline{u}/D_{12}$ such that a 2:1 or 1:2 step change in radius at the entrance of the diffusion tube results in an increment to the second temporal moment at the detector given by

$$\sigma_{\text{step}}^2 = a\left(\frac{R}{u}\right)^2 Pe^2 = \frac{4aR^4}{D_{12}^2}, \tag{24}$$

where R is the downstream radius. The parameter a is 7.22×10^{-6} for a divergent step and 4.18×10^{-5} for a convergent step. Although these results were obtained for tubes of radii about one order of magnitude smaller than those typically used in diffusion measurements, they should apply to the latter case because the Reynolds

numbers are similar, corresponding to a creeping flow regime. The result is that the contribution of such step changes is remarkably small. For example, with $R = 0.3$ mm and $D_{12} = 3 \times 10^{-9}$ m^2 s^{-1}, $\sigma^2_{\text{step}} = 1$ s^2 for a convergent step. Diameter ratios closer to unity will give rise to even smaller effects. The CFD calculations show that the local disturbances decay within a distance of a few hundred tube diameters downstream of the step change, so that the asymptotic limit expressed in Eq. 24 is typically achieved in practice. Therefore, it is recommended to restrict diameter ratios to the range of 0.5 to 2 and to ensure that σ^2_{step} as given by Eq. 24 is negligible.

3.6 Coiled Diffusion Tube

The diffusion column is typically many meters long and, to facilitate temperature regulation, it is invariably coiled. Coiling the tube can give rise to secondary flow effects that influence the dispersion. This effect has been studied by Nunge et al. [18] who obtained a series expansion in even inverse powers of $\lambda = R_c/R_0$, where R_c is the coil radius. Their result for the dimensionless dispersion coefficient $KD_{12}/(2\overline{u}_0 R_0)^2$ yields

$$K = \left[D_{12} + \frac{R_0^2 \overline{u}_0^2}{48 D_{12}}\right] + \frac{PeD_{12}}{\lambda^2}\left[\frac{\mathrm{Re}^4}{562^2 \times 40}\left\{\frac{-2569}{15840}Sc^2 + \frac{109}{43200}\right\}\right. \\ \left. + \frac{\mathrm{Re}^2}{41472}\left\{\frac{31}{60}Sc - \frac{25497}{13440}\right\} + \left\{\frac{419}{11520} + \frac{1}{4}\left(\frac{1}{Pe^2} + \frac{1}{192}\right)\right\}\right] + O\left(\lambda^{-4}\right). \quad (25)$$

Here, $Pe = Re \cdot Sc$ is the Peclet number as before, $Re = 2R_0\overline{u}_0\rho/\eta$ is the Reynolds number, $Sc = \eta/(\rho D_{12})$ is the Schmidt number, ρ is the density, and η is the dynamic viscosity. Under typical conditions, $Sc >> 1$, $10^0 \le Re \le 10^2$, $Pe >> 1$, and $K >> D$ in which case Eq. 27 simplifies to

$$K \approx \left(\frac{R_0^2 \overline{u}_0^2}{48 D_{12}} + D_{12}\right)\left[1 - \left(\frac{De^2 Sc}{653}\right)^2\right], \quad (26)$$

where $De = Re\sqrt{\lambda}$ is the Dean number. The corresponding contribution to the second temporal moment is given in Table 1. Assuming that the tube dimensions are characterized by length and volume, the corresponding time perturbation is zero.

3.7 Inlet and Outlet Tubing Runs

Often, there will be a length of tubing between the end of the diffusion column and the inlet of the detector module. Typically, there also will be a tubing run, possibly of a different internal diameter, within the detector module before the flow reaches the detector chamber. In some circumstances, it is necessary also to have an additional tubing run between the injector and the diffusion column, for example, when the latter is in a thermostat bath and the former is not. The results already assembled can be combined to estimate the effects of such tubing runs. Provided that abrupt

diameter changes have a negligible influence on dispersion, as indicated by the analysis above, the volumetric dispersion χ_2 is conserved across a junction. In a system comprising a diffusion column, designated by subscript $i=0$, and additional tubing sections, designated by subscript $i>0$, the total accumulated volumetric dispersion is

$$\chi_2 = \sum_{i=0}^{n} A_i^2 \left(\frac{\dot{V} L_i}{24\pi D_{12}^{(i)}} + \frac{2D_{12}^{(i)} V_i}{\dot{V}} \right) \tag{27}$$

where L_i is the length and A_i is the cross-sectional area of each tune section. Here, the diffusion coefficient may take different values in each section of tubing, corresponding to different (mean) temperatures. When the contribution of the terms $i>0$ is small, Eq. 27 may be approximated by

$$\chi_2 = \left(\frac{A_0^2 \dot{V} L_0}{24\pi D_{12}} \right) \left[1 + \sum_{i=1}^{n} \left(\frac{D_{12}}{D_{12}^{(i)}} \right) \left(\frac{R_i}{R_0} \right)^4 \left(\frac{L_i}{L_0} \right) \right] + A_0^2 \left(\frac{2D_{12} V_0}{\dot{V}} \right), \tag{28}$$

where axial dispersion in the additional tube sections has been ignored and $D_{12} = D_{12}^{(0)}$ is the diffusion coefficient at the column temperature. This shows that the combined volumetric dispersion is equivalent to extending the length of the dispersion tube by δL where [19]

$$\delta L = \sum_{i=1}^{n} \left(\frac{D_{12}}{D_{12}^{(i)}} \right) \left(\frac{R_i}{R_0} \right)^4 L_i. \tag{29}$$

Therefore, the influence of additional tubing sections will be small when they are short and have radii significantly less than that of the diffusion tube itself. The corresponding perturbations to the temporal mean and dispersion are given in Table 1.

3.8 Numerical Example

A complete Taylor Dispersion experiment is described by several geometric and flow parameters. Considering only the diffusion column itself, the primary variables are the internal volume V_0 and length L_0 of the column and the volumetric flow rate $\dot{V}$ of the mobile phase. Two useful constraints are a target value for the temporal mean $\bar{t}_0$ (e.g., $\bar{t}_0 = 30$ min) and a minimum value for the corresponding dimensionless temporal mean $\bar{\tau}_0$ (e.g., $\bar{\tau}_0 \leq 20$). Taking into account the largest diffusion coefficient values to be measured, these two criteria serve to constrain L_0 and V_0 (and hence R_0) for given $\dot{V}$. Next, one can consider the largest practical coiling radius that can be accommodated and adopting a constraint for De^2Sc (e.g., $De^2Sc \leq 100$) and considering also the density and viscosity of the mobile phase, one can choose a flow rate. Connecting tubes before and after the diffusion column should be as short as possible and their radii should be smaller than R_0 but not less than $R_0/2$. The geometry of the detector is typically fixed and it is then useful to evaluate all the perturbations listed in Table 1. The primary variables V_0, L_0, and $\dot{V}$ might then

be revised with the objective of limiting the perturbations to the temporal mean and variance to a few percent. Pressure drop across the flow path might be an additional factor to control in some situations, providing a constraint on the maximum flow rate.

For purposes of illustration, the perturbations detailed in Table 1 are enumerated in Table 3 for a particular set of apparatus parameters (defined in Table 4) with several diffusivities covering a wide range. These examples are representative of tracer diffusion measurements for different solutes in a solvent having the same density and viscosity as water at a temperature of 298.15 K and a pressure of 0.1 MPa. For simplicity, the injector, diffusion column, external tubing, and detector are all assumed to be at the same temperature so that only a single value of D_{12} appears. The geometry within the detector module (internal tubing and chamber) reflects the dimensions of a commercially available refractive index detector (RID) (Agilent, 1200 series). In fact, the influence of the tubing run within this module gives rise to the largest perturbations to the temporal mean and variance. The flow rate is kept constant in these examples at 0.15 mL·min^{-1} but could be adjusted to reduce the temporal variance perturbation. For example, for the highest diffusion coefficient considered, at which the relative temporal mean perturbation exceeds 3%, tripling the flow rate would have the effect of reducing the total relative temporal variance perturbation to 2% while keeping $De^2Sc < 35$.

4 Practical Implementation

For most purposes, commercially available HPLC or supercritical fluid chromatography equipment can be adapted to create a Taylor Dispersion Apparatus (TDA). On the other hand, commercial chromatography software is not usually suitable and bespoke control, data acquisition, and data analysis code are normally required.

4.1 Columns

Diffusion columns are usually fabricated from metals such as stainless steel or Hastelloy but might also be made in silica or from polymeric materials, such as PEEK or PTFE. The criteria are that the internal bore should be reasonably circular and uniform in radius and that neither of the fluid components should adsorb on, absorb into, permeate through or react with the tube material. Ideally, the diffusion column should be obtained as a single length of seamless tubing, although it may be acceptable to join sections if this is not possible. Here and elsewhere, zero dead volume chromatographic unions are recommended and sharp bends or kinks in the tube must be avoided.

Adsorption or absorption within the diffusion column may be difficult to detect in a TDA experiment. The theory of solute dispersion under steady laminar flow with adsorption, absorption, and/or chemical reactions has been examined in the literature [20, 21]. Golay considered rapid reversible adsorption [20], as in open-tube chromatography, and showed that peaks remain asymptotically Gaussian but exhibit

Table 3 Example calculations for the Taylor Dispersion apparatus detailed in Table 4

Flow and diffusion parameters						
Flow rate	$V/(m^3 \cdot s^{-1}) =$	1.67×10^{-9}	1.67×10^{-9}	1.67×10^{-9}	1.67×10^{-9}	1.67×10^{-9}
Density	$\rho/(kg \cdot m^{-3}) =$	997	997	997	997	997
Viscosity	$\eta/(Pa \cdot s) =$	0.89×10^{-4}	0.89×10^{-4}	0.89×10^{-4}	0.89×10^{-4}	0.89×10^{-4}
Diffusivity	$D/(m^2 \cdot s^{-1}) =$	1×10^{-9}	2×10^{-9}	5×10^{-9}	1×10^{-8}	2×10^{-8}
Reynolds number	Re =	4.8	4.8	4.8	4.8	4.8
Dean number	De =	0.2	0.2	0.2	0.2	0.2
Schmidt number	Sc =	892.7	446.3	178.5	89.3	44.6
Peclet number	Pe =	4244	2122	849	424	212
	$De^2Sc =$	33.6	16.8	6.7	3.4	1.7
Mean velocity	$\overline{u}/(m \cdot s^{-1}) =$	8.5×10^{-3}	8.5×10^{-3}	8.5×10^{-3}	8.5×10^{-3}	8.5×10^{-3}
Dispersion coefficient	$K/(m^2 \cdot s^{-1}) =$	9.4×10^{-5}	4.7×10^{-5}	1.9×10^{-5}	9.4×10^{-6}	4.7×10^{-6}
Dimensionless variable	$\zeta_0 =$	7.4×10^{-4}	3.7×10^{-4}	1.5×10^{-4}	7.4×10^{-5}	3.7×10^{-5}
Temporal variance	$\sigma_0^2 / s^2 =$	4602	2301	921	461	231
Temporal mean	$\overline{t_0}/s =$	1767	1767	1767	1767	1767
Dimensionless mean time	$\overline{\tau_0} =$	28.3	56.5	141	283	566
Peak skewness	$\beta =$	0.021	0.011	0.004	0.002	0.001
Temporal mean perturbations						
Injector	$\delta\overline{t}_{inj} =$	1.5	1.5	1.5	1.5	1.5
Detector	$\delta\overline{t}_{det} =$	2.4	2.4	2.4	2.4	2.4
Intercept	$\delta\overline{t}_{int} =$	0	0	0	0	0
Skewness	$\delta\overline{t}_{skew} =$	0.7	0.4	0.1	0.1	0.0
Coiling	$\delta\overline{t}_{coil} =$	0	0	0	0	0
Inlet tubing	$\delta\overline{t}_1 =$	8.8	8.8	8.8	8.8	8.8
Outlet tubing	$\delta\overline{t}_2 =$	8.8	8.8	8.8	8.8	8.8
Detector tubing	$\delta\overline{t}_3 =$	36.5	36.5	36.5	36.5	36.5
Total time perturbation	$\delta\overline{t}_{total} =$	58.8	58.4	58.2	58.1	58.1
	$\delta\overline{t}_{total} / \delta\overline{t}_0 =$	3.3%	3.3%	3.3%	3.3%	3.3%
Temporal variance perturbations						
Injector	$\delta\sigma^2_{inj} =$	0.8	0.8	0.8	0.8	0.8
Detector	$\delta\sigma^2_{det} =$	8.8	5.7	3.8	3.2	2.9
Intercept	$\delta\sigma^2_{int} =$	− 10.9	− 2.7	− 0.4	− 0.1	0.0
Skewness	$\delta\sigma^2_{skew} =$	4.7	1.2	0.2	0.0	0.0
Coiling	$\delta\sigma^2_{coil} =$	− 12.2	− 1.5	− 0.1	0.0	0.0
Inlet tubing	$\delta\sigma^2_1 =$	5.8	2.9	1.2	0.6	0.3
Outlet tubing	$\delta\sigma^2_2 =$	5.8	2.9	1.2	0.6	0.3
Detector tubing	$\delta\sigma^2_3 =$	73.6	36.8	14.7	7.4	3.7
Total variance perturbation	$\delta\sigma^2_{total} =$	76.3	45.9	21.2	12.4	7.9
	$\delta\sigma^2_{total} / \delta\sigma^2_0 =$	1.7%	2.0%	2.3%	2.7%	3.4%

Table 4 Dimensional details of the example Taylor Dispersion apparatus, where R is the radius, L is the length, V is the volume and R_{coil} is he coil radius

Element	R/m	L/m	V/m^3	R_{coil}/m
Injection loop	1.25×10^{-4}	0.102	5.01×10^{-9}	
Inlet tube	1.25×10^{-4}	0.3	1.47×10^{-8}	
Diffusion column	2.50×10^{-4}	15	2.95×10^{-6}	0.15
Outlet tube	1.25×10^{-4}	0.3	1.47×10^{-8}	
Detector internal tube	2.20×10^{-4}	0.4	6.08×10^{-8}	
Detector chamber	–	0.01	8.00×10^{-9}	

a modified dispersion coefficient. This indicates that adsorption may be a cause of undetected systematic error. Boddington and Clifford considered also absorption into the wall and reactions within the flowing medium [21], obtaining expressions for the modified dispersion coefficient and the mean retention time. Importantly, the latter generally differs from $V_0/\dot{V}$ and so, from a practical point of view, measurement of the temporal mean is an important check. Adsorption or absorption phenomena may also cause skewness of the distribution and this is an important point to consider in the validation of a TDA for a particular task. Obviously, if there is evidence of adsorption on, absorption into, or reaction with the tube material then an alternative material must be sought.

Both the length and volume of the tube must be known precisely, as they appear in Eq. 18 from which the diffusion coefficient is obtained. The tube volume can be determined gravimetrically by weighing it empty and then again when filled with, e.g., water. For the diffusion column specified in Table 4, the volume is almost 3 mL and this could be determined with a relative uncertainty below 0.1% by this method. In some cases, the length of the column may be measured directly with a tape measure. However, it must be stretched out in a perfectly straight line and this can be difficult for tubes longer than a few meters and for any malleable tube that has been tightly coiled. If the tube can be stretched out in this way then a relative uncertainty on the order of 0.1% should be achievable. If not, an alternative approach is to measure the retention time of an analyte in the assembled TDA under steady solvent flow. For this purpose, any common liquid solvent will suffice and a suitable analyte is one having a high diffusivity in the chosen solvent so that a sharp peak is obtained at the detector.

The diffusion column must be maintained at a constant temperature and this can be achieved with a suitable thermostatic fluid bath, a metal block thermostat or with a chromatographic oven. The former may be preferable at moderate temperatures as it should ensure the most uniform and stable temperature. A metal block (e.g., aluminum) can serve for both temperature regulation and as a former for coiling the tube. The diffusion column should always be wound on a former so that it follows a smooth helical path of a defined radius, without sharp bends or kinks that might disturb the flow pattern. Bruno reports achieving temperature stability and uniformity of ±0.015 K using a cylindrical aluminum former inside a modified chromatographic oven [22].

Temperature fluctuations are linked to flow rate perturbations through the thermal expansivity α of the mobile phase such that the volumetric flow rate is perturbed by $(\partial T/\partial t)\alpha V_0$ when the mean temperature T of the column is changing at a rate $(\partial T/\partial t)$. Therefore, a criterion for thermal stability can be written as $(\partial T/\partial t)\alpha V_0/\dot{V} \ll 1$. As an example, consider a typical organic liquid with $\alpha = 1.2 \times 10^{-3}$ K^{-1} so that in the scenarios detailed in Tables 3 and 4 one requires $(\partial T/\partial t) < 0.5 \times 10^{-3} K \cdot s^{-1}$ or about 1.7 $K \cdot h^{-1}$, for a relative flow rate perturbation $< 10^{-3}$. Another factor arises when the injection loop is outside the thermostat that encloses the diffusion column. In that case, the temperature of the mobile phase flowing into the diffusion column should equilibrate with the thermostat as rapidly as possible and this calls for good thermal anchoring between the tube and the thermostat medium.

Pressure drops across the flow system may be significant and some basic calculations are recommended to ensure that the mean column pressure is sufficiently well known, for example from an upstream measurement. When the mobile phase is a liquid, the influence of pressure drops is most likely negligible, although the situation may be different for a compressible supercritical fluid.

4.2 Injection System

Chromatographic injection valves offer the best method of injecting the sample. One may use either a four-port valve with an internal sample loop or a six-port valve with an external sample loop. The sample loop must be filled with a mixture or solution having a composition that differs slightly from that of the mobile phase. With mixtures or solutions that are liquid at atmospheric pressure and the filling temperature, the sample loop may be flushed and filled using a simple syringe, possibly automated with a computer-controlled syringe driver. If the mixture or solution is not a homogeneous fluid at atmospheric pressure and the filling temperature, but is so at higher pressure, then a pressurized reservoir is required and the waste port of the injection valve should be fitted with a back-pressure device to allow flushing without flashing [23]. In this situation, the pressure of the mobile phase should be greater than or equal to the loop filling pressure to avoid phase separation after injection. Loop volumes should be as small as possible, usually a few μL. When working with sparingly soluble gases or other solutes that will be present only at high dilution, larger loops may be needed to obtain a usable signal at the detector. Obviously, the relative magnitude of $\delta\sigma^2_{inj}$ as well as the signal-to-noise ratio must be considered when sizing the injection loop.

The injection valve may be located in the same thermostatic enclosure as the column, in which case the two can be directly connected. On the other hand, if the valve is not compatible with the column temperature then it must be sited outside of the thermostatic enclosure and a connecting tube used. Such a connecting tube should be as short as possible and be of smaller diameter than the diffusion column: half is recommended.

With a rotary chromatographic valve, sample injection is associated with a start time, at which the valve moves to the inject position, and a stop time, at which it returns to the fill position. The duration of the injection has in principle an influence on the initial conditions and, for the injector correction given in Table 1 to be valid, the duration should be a sufficient multiple of $V_{\mathrm{det}}/\dot{V}$ to ensure that the sample is largely swept onto the column. A multiple of 5 can be recommended.

4.3 Pumping System

When the mobile phase is liquid under ambient conditions, a normal HPLC pump is suitable for generating the required steady flow. A pulse dampener may be needed to help ensure smooth flow, although modern dual-piston pumps already produce a nearly pulseless flow. As a check, it is recommended to monitor the pressure at the outlet of the pump. In most cases, an in-line degasser is recommended to eliminate unwanted dissolved gases. A motorized syringe pump may be a suitable alternative, provided that it has sufficient capacity to support steady flow for the desired experimental duration. If the mobile phase is not homogeneous at ambient pressure than a pressurized delivery system is required. Some HPLC pumps can accept a pressurized inlet, as can certain syringe pumps. Bruno reports using a chilled dual-piston chromatographic pump fitted with a pulsation dampener to deliver liquid carbon dioxide at high pressures [24].

Depending upon the chosen pump, the volumetric flow rate at pump conditions will have an uncertainty of probably a fraction of a percent. This uncertainty might be reduced somewhat by calibration, for example, by collecting and weighing the amount of water pumped in a specified period of time. One should measure the temperature and the pressure at the pump conditions so that, knowing the volumetric flow rate there and the thermal expansivity of the mobile phase, one can determine the volumetric flow rate at column conditions. A large capacity syringe pump must be thermostatted precisely otherwise even quite small temperature fluctuations will create significant errors in flow rate. The criterion for temperature stability in this case is $(\partial T/\partial t)\alpha V_{\mathrm{pump}}/\dot{V} \ll 1$, where V_{pump} is the volume within the pump. If V_{pump} were 100 mL then, for the scenario detailed in Tables 3 and 4, one needs $(\partial T/\partial t) < 0.05\ \mathrm{K{\cdot}h^{-1}}$ for a relative flow rate perturbation $< 10^{-3}$. This analysis can be extended to incorporate any other volumes in the flow path, such as pressure sensors.

4.4 Detector Systems

Commercial chromatographic detectors are the norm. The most common for use in a TDA is the refractive index detector (RID) because of its near universal applicability; one only needs the refractive index to vary adequately with composition. Other composition monitors, such as ultraviolet–visible absorption detector (UV–VIS), diode array detector (DAD), fluorescence detector (FLD), electrical conductivity detector (ECD), or even a flame ionization detector (FID), may

be suitable for certain specific systems. These detectors can have much greater sensitivity to specific dilute analytes than does the more general RID.

RIDs and some other detectors have an internal thermostat to regulate the temperature of the detector cell and to pre-equilibrate the flow at that temperature. There is typically a length of tubing within the detector module through which the flow passes before entering the detector chamber itself. It is necessary to know the length and volume of this tubing and also the volume of the detector chamber, so that corrections can be applied. Approximate knowledge of the diffusion coefficient at the detector temperature is needed to estimate the tube correction.

In most cases, the detector must operate at or near to ambient pressure. A back-pressure device may be used to regulate the outlet pressure in cases where flashing would otherwise be a problem. If the diffusion column is to be operated at high pressure then a pressure reduction device is needed between the end of the column and the inlet to the detector module. Options for this include a back-pressure device and a small-bore restriction capillary. If the former is used then it should be of minimal dead volume. The latter is simple and effective but the column pressure depends upon flow rate. An interchangeable set of restrictor tubes can be used to cover a range of pressures [9]. When studying the tracer diffusion coefficients of organic components in a non-flammable supercritical fluid (e.g., CO_2), a restrictor tube and FID can be combined to good effect. In this case, the outlet from the restrictor tube flows directly into the FID [22, 25]. In the special case of tracer diffusion coefficient measurements of solutes in supercritical carbon dioxide, an entire supercritical fluid chromatograph may be adapted.

The detector is normally assumed to provide a linear response to composition changes, although this might not always be the case. While, for example, FIDs are linear over a wide range, RIDs are not. In order to check for linearity, experiments with differing concentration perturbations can be carried out. This can be achieved either by changing sample loop or by adjusting the composition of the injected aliquot. Non-linearity would be manifested by increasing relative deviations of the measured data from the working equation as the concentration perturbation increases.

4.5 Data Reduction and Analysis

Using a typical commercial chromatographic equipment, sample injection and signal collection may be automated fairly easily. It may be necessary to obtain proprietary information from the manufacturer to enable control of the pump and detector from a custom computer program; use of a custom control code will generally be more convenient than using software designed for chromatography. Typically, the detector signal is digitized every second and the data set for a single injection comprises $S(t)$, where t is the time measured from actuation of the sample injection valve and S is the signal returned by the detector, starting at injection and continuing until the signal has returned to baseline after elution of the sample.

Assuming a linear detector response factor α such that $\overline{c}_L(t) = S(t)/\alpha$, the measured data should conform to the equation

$$S(t) = \left[\frac{S_0}{\sqrt{(t/\bar{t})}}\right] \exp\left[\frac{-(t-\bar{t})^2}{2\sigma_0^2(t/\bar{t})}\right], \tag{30}$$

where S_0 is constant for a given injection. The parameters S_0, $\bar{t}$ and σ^2 may be obtained by a non-linear least-square fit to the $S(t)$ data. Typically, there is a non-zero baseline which exhibits some drift during the course of the measurement. Therefore, it is usual to include two additional parameters to describe the baseline as a linear function of time. The portion of the data set to be analyzed in this way should extend to both sides of the elution peak, sufficient to establish the baseline precisely.

Having obtained $\bar{t}$ and σ^2, the quantities $\bar{t}_0$ and σ_0^2 are determined as follows:

$$\bar{t}_0 = \bar{t} - \sum\nolimits_i \delta\bar{t}_i, \tag{31}$$

$$\sigma_0^2 = \sigma^2 - \sum\nolimits_i \delta\sigma_i^2, \tag{32}$$

where $\sum_i \delta\bar{t}_i$ is the sum of the temporal mean perturbations and $\sum_i \delta\sigma_i^2$ is the sum of the temporal variance perturbations based on the contributions listed in Table 1.

Finally, the diffusion coefficient D_{12} may be determined from Eq. 18. The time parameter $\bar{t}_0$ should accord with that calculated from Eq. 15 and this provides a check on the pump flow rate and the volume of the elements in the flow path from injector to detector. The residual deviations of the data from the fit also provide a check on the conformance of the experiment to the theory.

Traditionally, the data have been analyzed by computing directly the temporal moments. This remains an option, although the second-order expressions discussed by Alizadeh et al. [13] may need to be considered as the parameters $\bar{t}_0$ and σ_0^2 in Eq. 15 are not the exact temporal mean and variance. Evaluating also the third and fourth temporal moments can be recommended as a means of checking that the experimental data conform to the working equations.

4.6 Uncertainty

For purposes of evaluating the uncertainty (only), an approximate solution for D_{12} may be written:

$$D_{12} = \frac{V_0\bar{t}_0}{24\pi L_0\sigma_0^2} \approx \left(\frac{V_0\bar{t}}{24\pi L_0\sigma^2}\right)\left(1 - \frac{\delta\bar{t}_0}{\bar{t}} + \frac{\delta\sigma_0^2}{\sigma^2}\right). \tag{33}$$

The standard relative uncertainty of D_{12} is therefore obtained from the following relation

$$u_{\mathrm{r}}^2(D_{12}) \approx u_{\mathrm{r}}^2(\bar{t}) + u_{\mathrm{r}}^2(\sigma^2) + u_{\mathrm{r}}^2(V_0) + u_{\mathrm{r}}^2(L_0) + \left[u(\delta\bar{t}_0)/\bar{t}\right]^2 + \left[u(\sigma_0^2)/\sigma^2\right]^2, \quad (34)$$

where $u(X)$ is the standard uncertainty and $u_{\mathrm{r}}(X)$ is the standard relative uncertainty of quantity X. The standard relative uncertainties of $\bar{t}$ and σ^2 may be obtained in the non-linear regression from which these parameters are obtained; the standard relative uncertainties of V_0 and L_{o} are calculated based on the chosen methods of determination; finally, the standard uncertainties of the correction terms $\delta\bar{t}_0$ and $\delta\sigma_0^2$ must be estimated by considering the constituent parts, term by term.

The combined standard relative uncertainty of D_{12} is obtained finally by considering also the standard uncertainties of temperature T, pressure p, and mole fraction x for a binary mixture as follows:

$$u_{c,r}^2(D_{12}) = \left[\left(\frac{\partial \ln D_{12}}{\partial T}\right)u(T)\right]^2 + \left[\left(\frac{\partial \ln D_{12}}{\partial p}\right)u(p)\right]^2 + \left[\left(\frac{\partial \ln D_{12}}{\partial x}\right)u(x)\right]^2 + u_r^2(D_{12}). \quad (35)$$

The term in mole fraction may be dropped in a tracer diffusion coefficient measurement. The partial derivatives that appear here must be estimated in some way appropriate to the system under investigation. The pressure uncertainty should take account of the pressure drop along the length of the diffusion column.

5 Conclusion

The Taylor Dispersion method is one of the most reliable means of measuring diffusion coefficients in binary mixtures or solutions in the liquid or supercritical fluid regions. The theory, developed mainly by Taylor and Aris, is essentially complete and provides a sound basis for connecting raw experimental data with the desired diffusion coefficient and for estimating the uncertainty of the result. Commercial HPLC equipment can be adapted for the diffusion measurements in most cases, and this provides the simplest route to a working apparatus. Based on the analysis, one can conclude that a standard relative uncertainty of a mutual or tracer diffusion coefficient on the order of 1% is achievable, whereas 0.1% would be extremely challenging.

Supplementary Information The online version contains supplementary material available at https://doi.org/10.1007/s10765-024-03339-x.

Author contributions This paper was written entirely by the author based on a review of the literature and personal experience of the experimental technique described.

Funding No funds, grants, or other support were received for this study.

Data Availability No datasets were generated or analysed during the current study.

Declarations

Competing interest The author declares no competing interests.

References

1. P. Thiel, A. Paschke, J. Winkelmann, Ber. Bunsen-Ges. Phys. Chem. **96**, 750 (1992)
2. S. Kheirollahi, M. Zirrahi, H. Hassanzadeh, J. Chem. Eng. Data **67**, 2193 (2022)
3. L. Hao, D.G. Leaist, J. Chem. Eng. Data **41**, 210 (1996)
4. T. Funazukuri, C.Y. Kong, S. Kagei, Int. J. Thermophys. **22**, 1643 (2001)
5. S. Umezawa, A. Nagashima, The Journal of Supercritical Fluids **5**, 242 (1992)
6. G. Guevara-Carrion, S. Ancherbak, A. Mialdun, J. Vrabec, V. Shevtsova, Sci. Rep. **9**, 8466 (2019)
7. T. Umecky, T. Kuga, T. Funazukuri, J. Chem. Eng. Data **51**, 1705 (2006)
8. S.P. Cadogan, B. Mistry, Y. Wong, G.C. Maitland, J.P.M. Trusler, J. Chem. Eng. Data **61**, 3922 (2016)
9. S. Wang, T. Zhou, Z. Pan, J.P.M. Trusler, J. Chem. Eng. Data **68**, 1313 (2023)
10. N. Matsunaga, M. Hori, A. Nagashima, High Temperatures-High Pressures **25**, 185 (1993)
11. G. Taylor, Proc. R. Soc. Lond. Ser. A. R. Soc. Lond Ser. A **219**, 186 (1953)
12. R. Aris, Proc. R. Soc. Lond. Ser. A. R. Soc. Lond Ser. A **235**, 67 (1956)
13. A. Alizadeh, C.A. Nieto de Castro, W.A. Wakeham, Int. J. Thermophys. **1**, 243 (1980)
14. P.C. Chatwin, J. Fluid Mech. **43**, 321 (1970)
15. F. Gritti, G. Guiochon, J. Chromatogr. A **1218**, 4632 (2011)
16. P.K. Dasgupta, C.P. Shelor, A.F. Kadjo, K.G. Kraiczek, Anal. Chem. **90**, 2063 (2018)
17. A. Moussa, K. Broeckhoven, G. Desmet, J. Chromatogr. A **1688**, 463719 (2023)
18. R.J. Nunge, T.S. Lin, W.N. Gill, J. Fluid Mech. **51**, 363 (1972)
19. C. Secuianu, G.C. Maitland, J.P.M. Trusler, W.A. Wakeham, J. Chem. Eng. Data **56**, 4840 (2011)
20. M.J.E. Golay, in *Gas Chromatography*. ed. by D.H. Destry (Butterworths, London, 1958), p.35
21. T. Boddington, A.A. Clifford, P. Gray, Proc. R. Soc. Lond. A Math. Phys. Sci.Lond A: Math. Phys. Sci. **389**, 179 (1983)
22. T.B. Bruno, J. Res. Natl. Inst. Stand. Technol. **94**, 105 (1989)
23. S.P. Cadogan, G.C. Maitland, J.P.M. Trusler, J. Chem. Eng. Data **59**, 519 (2014)
24. M. Bruno, F.R. Massaro, L. Pastero, E. Costa, M. Rubbo, M. Prencipe, D. Aquilano, Cryst. Growth Des. **13**, 1170 (2013)
25. C.M. Silva, E.A. Macedo, Ind. Eng. Chem. Res. **37**, 1490 (1998)